Electronic Supplementary Material (ESI) for Physical Chemistry Chemical Physics.

Supplementary Information

Principal molecular axis and transition dipole moment orientations in liquid crystal systems: an assessment based on studies of guest anthraquinone dyes in a nematic host

Mark T. Sims, Laurence C. Abbott, Stephen J. Cowling, John W. Goodby and
John N. Moore*
Department of Chemistry, University of York, Heslington, York YO10 5DD, UK

Principal molecular axes of the dyes

The principal moment of inertia axes, $\mathbf{I}_i$, calculated for the molecular geometries in the MD simulations have unambiguous orientations but their directions are arbitrary. In order to use these principal moment of inertia axes to define a molecular frame from which to determine the orientations of the axes, $\mathbf{a}_{\mathrm{MOI}}$, it was necessary to ensure that the directions of these axes, $\mathbf{I}_i$, remained consistent within each dye molecule during the simulation.

For each molecule, the directions of $\mathbf{I}_a$ and $\mathbf{I}_b$ were defined as those that gave positive projections onto vectors defined by the substituent atom at the 1- position for 15SB3, 15NB3 and 15NB3OH and at the substituent atom at the 2- position for 26B3 and 26B3OH, relative to the molecular centre of mass. The direction of $\mathbf{I}_c$ was then defined such that the three principal moment of inertia axes gave a right-handed coordinate system.

The coefficients, c_a, c_b and c_c, of the axes, $\mathbf{a}_{\mathrm{MOI}}$, defined against the principal moment of inertia axes as described above, are given for all the dyes in Table S1.

Table S1 Coefficients, c_i, of the axes, $\mathbf{a}_{\mathrm{MOI}}$, of the dyes, determined in accordance with eqn 11 in the main text and normalised.

Dye	c_a	c_b	c_c
15SB3	0.9687	0.2476	0.0167
15NB3	0.9892	0.1460	0.0109
15NB3OH	0.9963	−0.0833	0.0198
26B3	0.9922	−0.1236	0.0133
26B3OH	0.9978	−0.0661	−0.0072

MD simulations of the E7 host alone

Figures S1 and S2 show results from the MD simulations of E7 alone, using either pseudo-nematic or isotropic starting geometries, respectively. These figures relate to Table 3 in the main text.

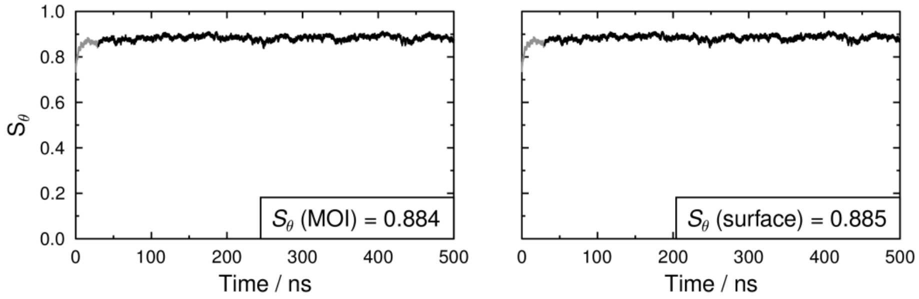

Fig. S1 Molecular order parameters, S_θ, calculated over all molecules at each trajectory step for the simulation of 400 component molecules of E7 alone, starting from a pseudo-nematic geometry and using the minimum MOI axes (left) and the surface tensor axes (right). Insets give S_θ values obtained from averaging over 30-500 ns, as shown by the ranges plotted in black.

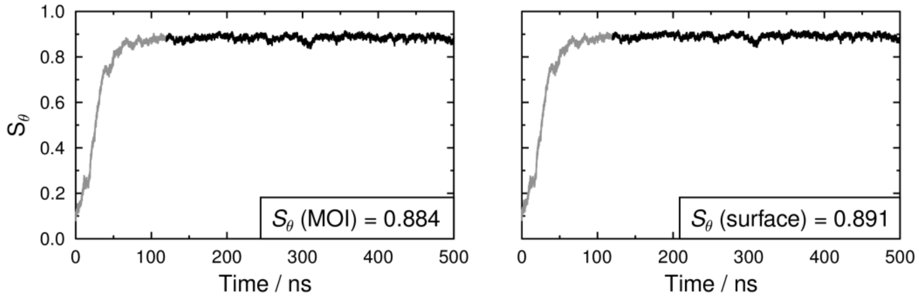

Fig. S2 Molecular order parameters, S_θ, calculated over all molecules at each trajectory step for the simulation of 256 component molecules of E7 alone, starting from an isotropic geometry and using the minimum MOI axes (left) and the surface tensor axes (right). Insets give S_θ values obtained from averaging over 120-500 ns, as shown by the ranges plotted in black.

Dihedral angle analysis of the dyes

The dihedral angle population distributions of 15SB3, 15NB3 and 15NB3OH presented in Fig. 11 of the main text were determined according to the following procedure. The populations about the dihedral angles, ψ_1, defined by atoms 1-2-X-3 in Fig. S3 and the equivalent atoms in the other half of the molecule were determined for each dye molecule for each trajectory step of each MD simulation and summed before normalising the total population to 1 to give the plots labelled ψ_1 in Fig. 11 of the main text. The populations about the dihedral angles, ψ_2, defined by atoms 2-X-3-4 in Fig. S3 were determined in the same way but, after summing over all molecules, the populations at angles ψ_2 >180° were added to the populations at the equivalent angles at ψ_2 < 180° before normalising to give the distributions labelled ψ_2 for the 0-180° range shown in Fig. 10 of the main text; angles at ψ_2 and ψ_2 + 180° are equivalent structures due to the equivalence of atoms 4a and 4b.

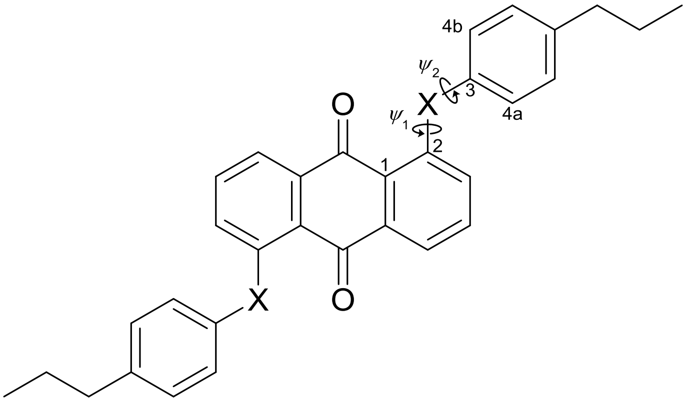

Fig. S3 Generic 1,5-disubstituted anthraquinone structure showing the atom labelling used to define the dihedral angles about the substituent linking group, X.

The dihedral angle population distributions of 26B3 and 26B3OH, also presented in Fig. 11 of the main text, were determined using the same method as that described above to determine the distributions of ψ_2 for 15SB3, 15NB3 and 15NB3OH.

The subsequently determined bin limits for matching the conformers of the dyes from the MD simulations with those for which TDM vector orientations had been calculated for the model structures are given in Table S3.

Table S3 Limits of the bins used to assign dye conformers in the MD simulations to those of the model structures for which TD-DFT calculations had been run. The values correspond to the boundaries between shaded regions in Fig. 11 in the main text.

Dye		Dihedral bin limits / °										
15SB3	ψ_1	0	167.25	175.75	184.25	192.75	360					
	ψ_2	0	67.50	82.50	97.50	112.50	180					
15NB3	ψ_1	0	158.25	172.75	187.25	201.75	360					
	ψ_2	0	47.25	75.75	104.25	132.75	180					
15NB3OH	ψ_1	0	156.00	172.00	188.00	204.00	360					
	ψ_2	0	47.75	72.25	104.75	134.25	180					
26B3	ψ_1	0	15.75	27.25	38.75	50.25	90	129.75	141.25	152.75	164.25	180
26B3OH	ψ_1	0	28.75	40.25	51.57	63.25	90	116.75	128.25	139.75	151.25	180

Model structures for TD-DFT calculations

TD-DFT calculations were carried out for a range of optimised model structures in order to assess which could be used as satisfactory models of the dyes to reduce the computational expense of calculating TDM orientations for representative structures of the dyes explored in the MD simulations.

The wavelengths, λ, and oscillator strengths, f, of the visible transitions calculated for the optimised model structures and for the optimised structures of dyes themselves are listed in Table S4, where the numerical suffixes denote the number of carbon atoms in the terminal alkyl chains. Table S4 also lists the values of n_{AQ}, n_{CO} and n_{ORTH}, which correspond to the projections of the TDM unit vectors onto the AQ, CO and ORTH axes, respectively, as defined in Fig. 12 in the main text, which enable the orientations of the calculated TDMs to be compared between structures.

The results show that the alkyl chains have little effect on the calculated visible transitions for 15SB3, 15NB3 and 15NB3OH, and that the structures with hydrogen atoms replacing the propyl groups provide a satisfactory model, whereas methyl groups are required to provide satisfactory models to replicate the visible transitions for 26B3 and 26B3OH. The transitions calculated for these selected model structures were found to arise from essentially the same orbital contributions as those calculated for the dyes.

Table S4 Calculated wavelengths, λ, and oscillator strengths, f, of the allowed visible electronic transitions of the propyl-substituted dyes and their hydrogen and methyl substituted analogues, along with their normalised projections onto the AQ, CO and ORTH axes.

Dye	λ / nm	f	n_{AQ}	n_{CO}	n_{ORTH}
15SB3	453	0.27	0.92	0.40	0.00
15SB0	451	0.25	0.92	0.41	0.00
15NB3	552	0.35	0.90	0.45	0.04
15NB0	542	0.32	0.91	0.43	0.05
15NB3OH	634	0.55	0.91	0.41	0.06
15NB0OH	625	0.49	0.92	0.39	0.06
26B3	390	0.29	0.89	0.45	0.01
26B0[a]	-	-	-	-	-
26B1	389	0.23	0.88	0.46	0.01
26B3OH	492	0.57	0.95	0.27	0.01
26B0OH	478	0.49	0.96	0.28	0.00
26B1OH	491	0.53	0.95	0.30	0.00

[a] no visible transitions calculated with orbital contributions comparable to that of the dye